Weak-microcavity organic light-emitting diodes with improved light out-coupling

Sang-Hwan Cho[1,2*], Young-Woo Song[2], Joon-gu Lee[2], Yoon-Chang Kim[2], Jong Hyuk Lee[2], Jaeheung Ha[2], Jong-Suk Oh[2], So Young Lee[2], Sun Young Lee[2], Kyu Hwan Hwang[2], Dong-Sik Zang[2] and Yong-Hee Lee[1]

[1] Department of Physics, KAIST, Daejeon 305-701, Korea
[2] Material Laboratory, Corporate Research and Development Center, Samsung SDI Co., Ltd., Yongin, Gyeonggi-do 446-577, Korea
**Corresponding author: cho0825@kaist.ac.kr*

Abstract: We propose and demonstrate weak-microcavity organic light-emitting diode (OLED) displays with improved light-extraction and viewing-angle characteristics. A single pair of low- and high-index layers is inserted between indium tin oxide (ITO) and a glass substrate. The electroluminescent (EL) efficiencies of discrete red, green, and blue weak-microcavity OLEDs are enhanced by 56%, 107%, and 26%, respectively, with improved color purity. Moreover, full-color 128×160 passive-matrix bottom-emitting OLED displays are fabricated by employing low-index layers of two thicknesses. As a display, the EL efficiency of white color was 27% higher than that of a conventional OLED display.

OCIS codes: (220.0220) Optical design and fabrication; (230.1480) Bragg reflectors; (230.3670) Light-emitting diodes.

References and links

1. V. Bulovic, V. B. Khalfin, G. Gu, P. E. Burrows, D. Z. Garbuzov, and S. R. Forrest, "Weak microcavity effects in organic light-emitting devices," Phys. Rev. B **58,** 3730-3740 (1998).
2. S. Möller and S. R. Forrest, "Improved light out-coupling in organic light emitting diodes employing ordered microlens arrays," J. Appl. Phys. **91**, 3324-3327 (2002).
3. M. -K. Wei and I-L. Su, "Method to evaluate the enhancement of luminance efficiency in planar OLED light emitting devices for microlens array," Opt. Express **12**, 5777-5782 (2004).
4. C. F. Madigan, M. -H. Lu, and J. C. Strurm, "Improvement of output coupling efficiency of organic light-emitting diodes by backside substrate modification," Appl. Phys. Lett. **76**, 1650-1652 (2000).
5. T. Yamasaki, K. Sumioka, and T. Tsutsui, "Organic light-emitting device with an ordered monolayer of silica microspheres as a scattering medium," Appl. Phys. Lett. **76**, 1243-1245 (2000).
6. B. J. Matterson, J. M. Lupton, A. F. Safonov, M. G. Salt, W. L. Barnes, and I. D. W. Samuel, "Increased efficiency and controlled light output from a microstructured light-emitting diode," Adv. Mater. **13**, 123-127 (2001).
7. P. A. Hobson, S. Wedge, J. A. E. Wasey, I. Sage and W. L. Barnes, "Surface plasmon mediated emission from organic liget-rmitting diodes," Adv. Mater **14**, 1393-1396 (2002).
8. T. Tsutsui, M. Yahiro, H. Yokogawa, K. Kawano, and M. Yokoyama, "Doubling Coupling-Out Efficiency in Organic Light-Emitting Devices using a Thin Silica Aerogel Layer," Adv. Mater. **13**, 1149-1152 (2001).
9. Y. -J. Lee, S. -H. Kim, J. Huh, G. -H. Kim, Y. -H. Lee, S. -H. Cho, Y. -C. Kim, and Y. R. Do, "A high-extraction-efficiency nanopatterned organic light-emitting diode," Appl. Phys. Lett. **82**, 3779-3781 (2003).
10. Y. R. Do, Y. C. Kim, Y .-W. Song, C. -O Cho, H. Jeon, Y. -J. Lee, S. -H. Kim, and Y. -H. Lee, "Enhanced Light Extraction from Organic Light-Emitting Diodes with 2D SiO_2/SiN_x Photonic Crystals," Adv. Mater **15**, 1214-1218 (2003).
11. Y. -J. Lee, S. -H. Kim, G. -H. Kim, Y. -H. Lee, S. -H. Cho, Y. -W. Song, Y. -C. Kim, and Y. R. Do, "Far-field radiation of photonic crystal organic light-emitting diode," Opt. Express **13**, 5864-5870 (2005).
12. Y. -C. Kim, S. -H. Cho, Y. -W. Song, Y. -J. Lee, Y. -H. Lee, and Y. R. Do, "Planarized SiN_x/spin-on-glass photonic crystal organic light-emitting diodes," Appl. Phys. Lett. **89**, 173502 (2006).
13. N. Takada, T. Tsutsui, and S. Saito, "Control of emission characteristics in organic thin-film electroluminescent diodes using an optical-microcavity structure," Appl. Phys. Lett. **63**, 2032-2034 (1993).
14. T. Tsutsui, N. Takada, S. Saito and E. Ogino, "Sharply directed emission in organic electroluminescent diodes with an optical-microcavity structure," Appl. Phys. Lett. **65**, 1868-1870 (1994).
15. R. H. Jordan, L. J. Rothberg, A. Dodabalapur, and R.E. Slusher, "Efficiency enhancement of microcavity organic light emitting diodes," Appl. Phys. Lett. **69**, 1997-1999 (1996).

#96549 - $15.00 USD Received 23 May 2008; revised 17 Jul 2008; accepted 31 Jul 2008; published 6 Aug 2008

16. S. Tokito, K. Noda, and Y. Taga, "Strongly directed single mode emission from organic electroluminescent diode with a microcavity," Appl. Phys. Lett. **68**, 2633-2635 (1996).
17. S. Tokito, T. Tsutsui and Y. Taga, "Microcavity organic light-emitting diodes for strongly directed pure red, green, and blue emissions," J. Appl. Phys. **86**, 2407-2411 (1999).
18. A. Taflove and S. Hagness, *Computational Electrodynamics: the Finite-Difference Time-Domain Method* (Artech House, Boston, 2005).

1. Introduction

Organic light-emitting diodes (OLEDs) have attracted much attention because of their desirable characteristics, which include a wide viewing angle and a fast response. However, more than 80% of the emitted light is trapped and wasted in the high-index layers as a result of the total internal reflection [1] in conventional OLED structures. Accordingly, light extraction represents one of the hottest issues in this field and various techniques, such as the formation of microlens arrays [2-4] or microstructures [5-7] at the glass surface or the insertion of aerogel films [8], have been applied to approach this problem. The effect of incorporating a 2D SiO_2/SiN_x photonic-crystal layer was also investigated [9-12], whereby a 1.8-fold improvement was observed. However, nontrivial large-scale fabrication problems prevented real deployments in this area.

Recently, a few groups [13-17] introduced dielectric Bragg mirrors into the OLED structures, thus achieving improved emission characteristics and spectral narrowing. However, excessive microcavity effects generated undesirable angular-emission characteristics. In this article, we propose an OLED structure with a weak microcavity that delivers both a high light-extraction efficiency and wide viewing-angle characteristics.

2. Design and simulation

A schematic representation of the proposed weak-microcavity OLED (WMOLED) is shown in Fig. 1. A conventional OLED consists of a multilayer sandwich composed of a glass substrate, indium tin oxide (ITO), organic layers, and a metal cathode. The organic layers typically consist of an electron-injection layer (EIL), an electron-transport layer (ETL), an emitting-material layer (EML), a hole-transport layer (HTL), and a hole-injection layer (HIL). In our structure, a pair of low- and high-index layers is added between ITO and the glass substrate in order to increase the top reflectivity. The microcavity is weakly formed by the Al cathode mirror and one pair of low- and high-index dielectric layers. Three regions of high and low indices are indicated in Fig. 1. The indices of the organic and ITO layers are considered high. If each layer satisfies the resonant condition proposed in Eq. (1), the reflectivity is optimized for λ. Here n and d represent the refractive index and the thickness of the layer, respectively, whereas m is the mode number and λ is the wavelength of light.

$$\sum_i n_i d_i = \frac{(2m-1)\lambda}{4} \tag{1}$$

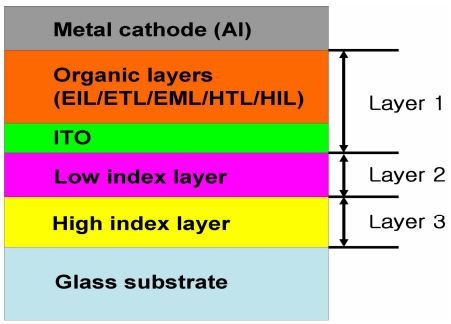

Fig. 1. Schematic representation of a weak-microcavity OLED.

#96549 - $15.00 USD Received 23 May 2008; revised 17 Jul 2008; accepted 31 Jul 2008; published 6 Aug 2008

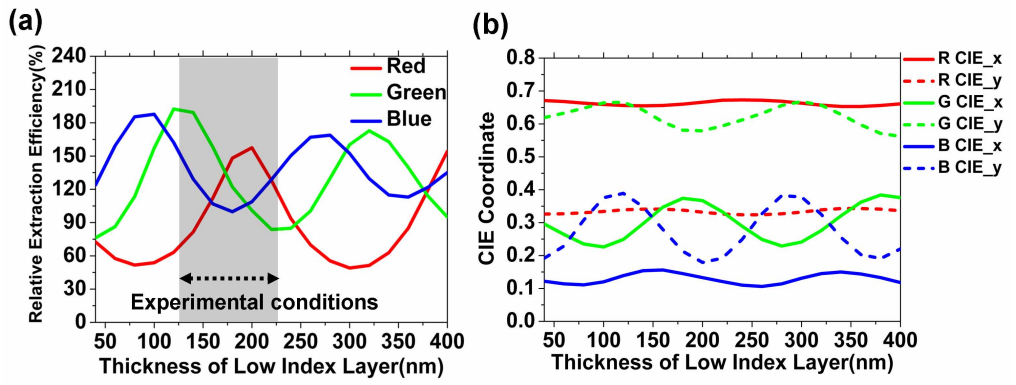

Fig. 2. (a). Relative extraction efficiency (T_H= 60 nm and T_{ITO}= 60 nm). The shaded area represents the thickness span tested in the real experiments (shown in Fig. 3). (b) CIE 1931 color coordinates of the WMOLEDs as a function of T_L.

The finite-difference time-domain (FDTD) method [18] was employed to investigate the extraction efficiencies, viewing-angle characteristics, and the spectra of incoherent LED emission. The extraction efficiency depends on T_{ITO}, T_L, and T_H, that is, the thicknesses of the ITO, the low-index, and the high-index layers, respectively. The thicknesses of the organic layers were borrowed from conventional specifications. In our computations, we used T_{ITO} values ranging between 40 and 200 nm, because it is known that the electrical properties of the OLEDs are not noticeably degraded within this thickness span. The refractive indices of the low- and high-index layers in Fig. 1 are assumed to be 1.4 and 2.1, respectively. Note that the optimal conditions for each color are widely scattered. In other words, each color needs to be designed and fabricated differently, and the fabrication of real full-color OLED displays becomes very complicated.

To simplify the fabrication processes, we fix both T_{ITO} and T_H to 60 nm for all three colors. In this case, the optical thicknesses of the high-index layers are $0.2\lambda_r$ for Red (R), $0.24\lambda_g$ for Green (G), and $0.27\lambda_b$ for Blue (B), where λ_r is 620 nm, λ_g is 530 nm, and λ_b is 470 nm. Although the resonant conditions [Eq. (1)] are not fully satisfied under the above specifications, noticeable increments in the device efficiency can still be obtained for all the colors. The weak-microcavity effect is then adjusted further by tuning T_L as shown in Fig. 2(a).

In order to appropriately evaluate the performance of an OLED, both the chromaticity and the extraction efficiency should be taken into account. The perceived color is usually expressed by the chromaticity coordinates developed by the Commission International De'Eclairage (CIE), 1931. For an enhanced color gamut, a larger x and a smaller y coordinate of red are required in the CIE 1931 diagram; for green, a smaller x and a larger y coordinate are necessary; and for blue, a smaller x and a smaller y coordinate are preferred. The CIE 1931 coordinates of conventional R, G, and B OLEDs are (0.668, 0.330), (0.315, 0.617), and (0.128, 0.241), respectively.

In the case of blue, although the out-coupling efficiency is the highest (namely, 188%) when T_L is 100 nm, the color becomes greenish-blue (0.120, 0.376) and unacceptable. Considering both the chromaticity and the out-coupling efficiency, a T_L value of 60 nm is optimal. In this case, the out-coupling efficiency and the color coordinate are 160% and (0.114, 0.229), respectively. Two optimal designs are summarized in Table 1. Although Layer 1 (organic layers + ITO) and Layer 2 (low-index layer) do not satisfy the resonant condition of Eq. (1) independently, the sum of these two layers is adjusted to be a multiple of the half-wavelength. Design A represents the case of the mode number two for all three colors, whereas design B represents the situation that reflects realistic fabrication constraints, where the mode number is three for blue. A T_L value of 220 nm (instead of 60 nm) was favored because of the electrical-shortage problem.

#96549 - $15.00 USD Received 23 May 2008; revised 17 Jul 2008; accepted 31 Jul 2008; published 6 Aug 2008

Table 1. Two optimal WMOLED designs expressed in optical thicknesses. Note the two different values of the low-index layers for the blue pixels (design A: T_L=60nm, design B: T_L=120nm). For the red and green pixels, the T_L values are fixed at 200 and 120 nm, respectively. T_{ITO}= T_H= 60 nm.

	Layer 1 (OL+ITO)	Layer 2 (Low-index)	Layer 3 (High-index)
Red (620nm)	$0.56\lambda_r$	$0.45\lambda_r$	$0.20\lambda_r$
Green (530nm)	$0.69\lambda_g$	$0.32\lambda_g$	$0.24\lambda_g$
Blue (470nm)	$0.82\lambda_b$	$0.18\lambda_b$/$0.66\lambda_b$	$0.27\lambda_b$

3. Mono-color OLED: Fabrication and results

We fabricated mono-color OLED samples with an active area of 2×2 mm^2. A TiO_2-based spin-on-glass (SOG, n=2.1) material was applied on a glass substrate. The coated SOG film was then soft-baked and fully cured (at 400℃) under nitrogen atmosphere for an hour. After this, a second layer of silsesquioxane-based SOG (n=1.4) was spin-coated and cured under the same conditions. Then, the ITO layer was deposited—using a magnetron sputtering system with no intentional heating—and organic layers corresponding to HIL, HTL, EML, and ETL as well as an LiF film (as EIL) and an aluminum metal cathode were evaporated simultaneously to fabricate both the reference and test devices. The chemical name of each organic layer is summarized in Table 2.

The measured extraction characteristics of the fabricated OLEDs agree well with the predicted FDTD behavior [see Fig. 3(a)], and the measured chromaticity also follows the theoretical prediction faithfully [see Fig. 3(b)]. In addition, we carried out electroluminescence (EL) analyses to confirm the microcavity effects. Figure 4 shows the EL efficiency–current density characteristics of a WMOLED measured from the direction normal to the substrate. The red, green, and blue EL efficiencies are enhanced by 56%, 107%, and 26%, respectively. Here the T_Ls values for R, G, and B (design B) are 200, 120, and 220 nm, respectively.

The emission spectra of the WMOLEDs are narrower than those of the reference OLEDs [see Fig. 5(a)]. The color purity is also improved for all three colors, as summarized in Table 3. We also emphasize that all the WMOLEDs show only small variations in their spectra [see Figs. 5(b)–5(d)] and their angular radiation patterns [see Figs. 6(a)–6(c)] over a large angular span. In other words, our WMOLED structure provides both a high efficiency and a wide angular tolerance.

Table 2. Chemical name of each organic layer and its thickness.

Organic layer	Material	Thickness (nm)
HIL	N,N′-diphenyl-N,N′-bis-[4-(phenyl-m-tolyl-amino)-phenyl]-biphenyl-4,4′-diamine (DNTPD)	60
HTL	N,N′-di(1-naphthyl)-N,N′-diphenylbenzidine (NPB)	20
R-EML	Rubrene doped with 3% 10-(2-Benzothiazolyl)-2, 3, 6, 7-tetrahydro-1, 1, 7, 7-tetramethyl-1H, 5H, 11H-(1)-benzopyropyrano(6, 7-8-i, j)quinolizin-11-one (DCJTB)	40
G-EML	Tris(8-hydroxyquinoline)aluminium (Alq3) doped with 1% 10-(2-Benzothiazolyl)-2, 3, 6, 7-tetrahydro-1, 1, 7, 7-tetramethyl-1H, 5H, 11H-(1)-benzopyropyrano(6, 7-8-i, j)quinolizin-11-one (C545T)	40
B-EML	Distyrylanthracene (DSA) doped with 5% anthracenedipenylamine (DSAamine)	40
ETL	Alq3	20
EIL	LiF	1

#96549 - $15.00 USD Received 23 May 2008; revised 17 Jul 2008; accepted 31 Jul 2008; published 6 Aug 2008

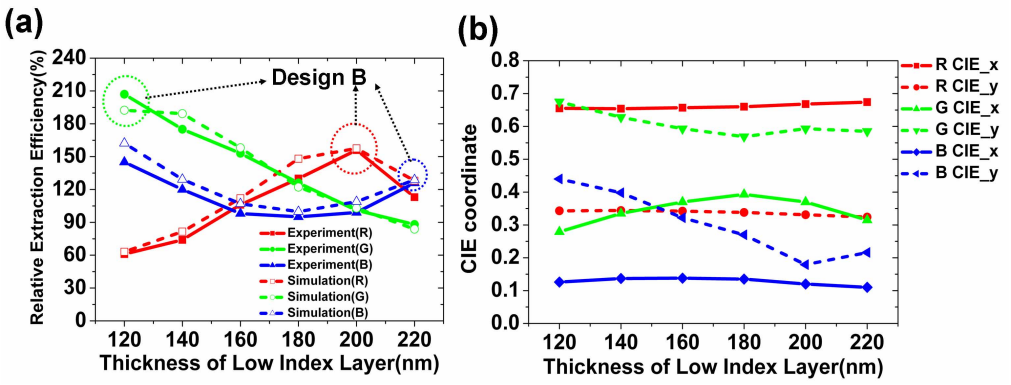

Fig. 3. (a). Measured extraction efficiencies as a function of T_L. The dashed lines represent the results of the FDTD computation. Design B is denoted by dashed circles. (b) CIE color coordinates of the fabricated WMOLEDs.

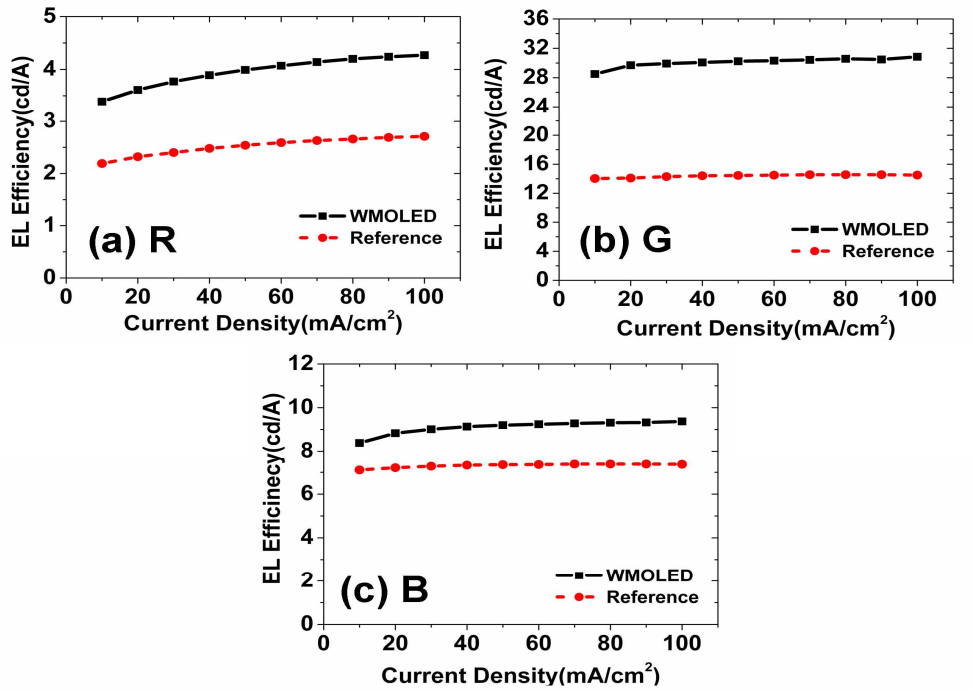

Fig. 4. EL efficiency–current density characteristics of the WMOLEDs at design B. The solid and dashed lines represent the WMOLEDs and conventional OLEDs, respectively.

#96549 - $15.00 USD Received 23 May 2008; revised 17 Jul 2008; accepted 31 Jul 2008; published 6 Aug 2008

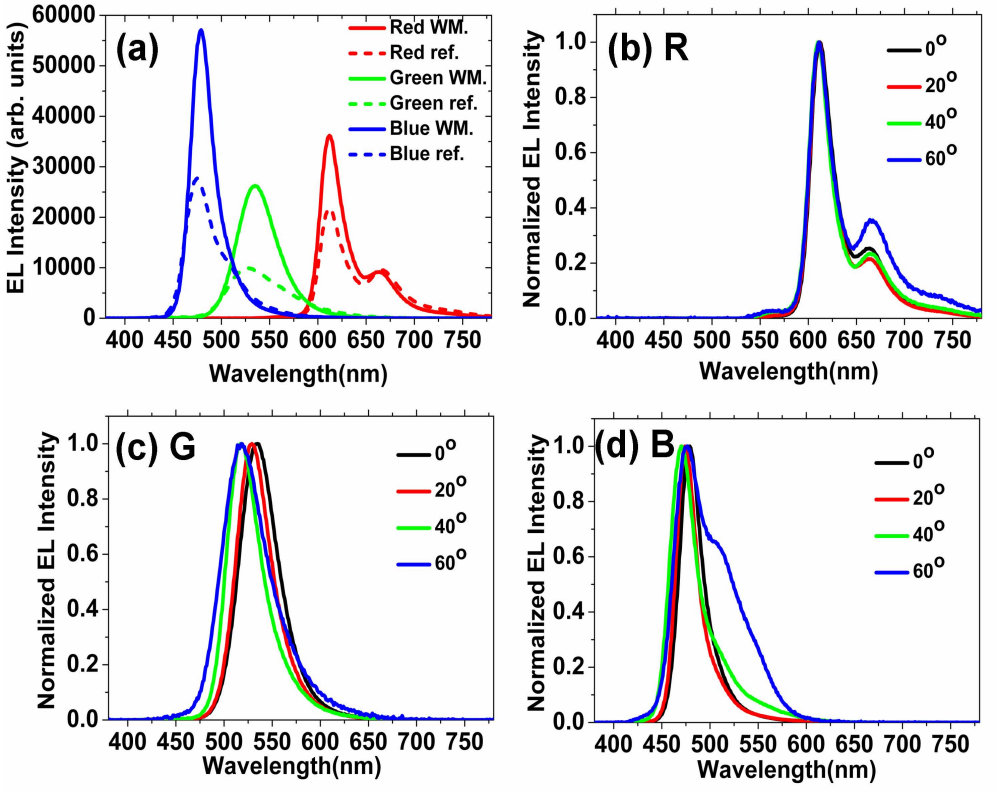

Fig. 5. (a). Comparison of EL spectra measured at the normal direction. The solid lines represent the spectra of the WMOLEDs and the dashed lines represent those of the conventional OLEDs. (b)–(d) Viewing-angle characteristics of red, green, and blue WMOLEDs.

Table 3. Comparison of current efficiencies and CIE 1931 coordinates at 100 mA/cm^2.

	WMOLED			Conventional OLED		
	Efficiency (cd/A)	CIE_x	CIE_y	Efficiency (cd/A)	CIE_x	CIE_y
Red	4.27	0.668	0.331	2.71	0.668	0.330
Green	30.85	0.279	0.675	14.5	0.315	0.617
Blue	9.37	0.110	0.216	7.37	0.128	0.241

#96549 - $15.00 USD Received 23 May 2008; revised 17 Jul 2008; accepted 31 Jul 2008; published 6 Aug 2008

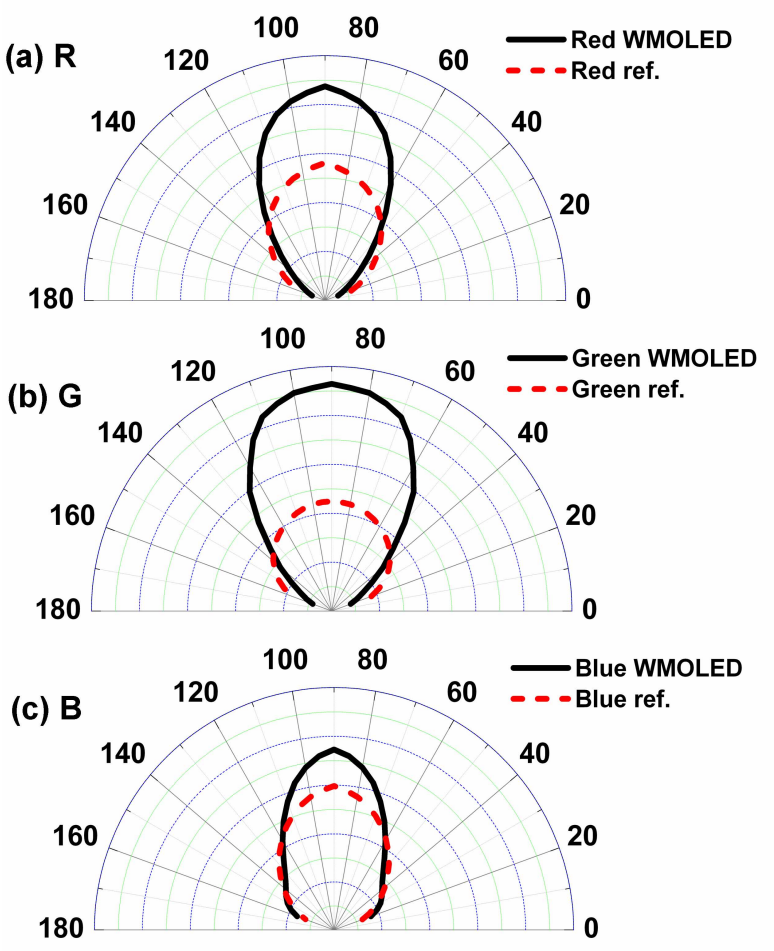

Fig. 6. Angular-radiation patterns of WMOLEDs.

4. Full-color passive matrix OLED: Fabrication and results

To test our proposal in a real display, we fabricated full-color passive-matrix bottom-emitting OLED displays with 128×160 pixels [see Fig. 7(a)]. As stated above, we were able to optimize the weak microcavity effect by tuning T_L differently for each color pixel. The previous design B represented the optimal performance. However, in this case, color-dependent three-step etching processes become troublesome. In order to alleviate fabrication burdens, two different T_L values are chosen.

Note in Table 3 that the performance of the green WMOLED is excellent in comparison to those of the red and blue WMOLEDs. Thus, we decided to focus on the red and blue subpixels, at the expense of the green subpixels, to realize a better white color display. The red and blue subpixels were fabricated at the optimal T_L values, whereas for the green subpixels, the T_L value for red was used. The final T_L values are 200 and 220 nm for the red/green and blue subpixels, respectively. This design is realized by simple one-step 20-nm etching of the low-index layer of red/green subpixels. The EL efficiency of white color in the WMOLED display is 27% higher than that of a conventional OLED display. In this case, the enhanced EL efficiencies of red, green, and blue colors correspond to 56%, 3%, and 26%, respectively. Images of the fabricated displays are shown side-by-side in Fig. 7(b) for comparison.

#96549 - $15.00 USD Received 23 May 2008; revised 17 Jul 2008; accepted 31 Jul 2008; published 6 Aug 2008

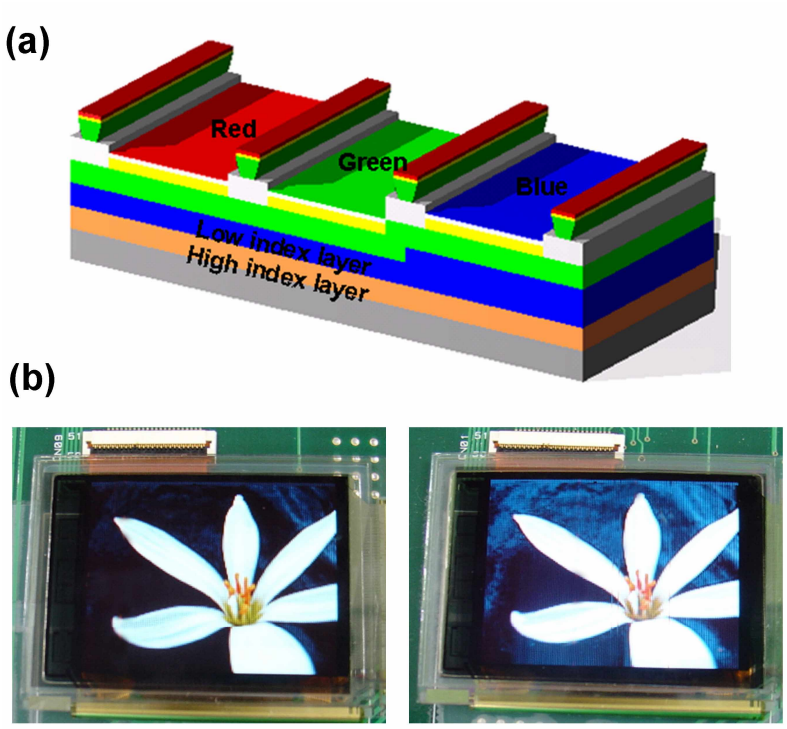

Fig. 7. (a). Schematic representation of a fabricated full-color passive-matrix bottom-emitting WMOLED display. (b) Comparison of 128×160 displays based on conventional OLEDs (left) and WMOLEDs (right)

5. Summary

In summary, the proposed OLED—supported by weak microcavity effects—demonstrated both enhanced light-extraction and wide viewing-angle characteristics. Simple introduction of a pair of dielectric layers improved the efficiencies of red, green, and blue colors by 56%, 107%, and 26%, respectively. We also fabricated full-color 128×160 passive-matrix bottom-emitting WMOLED displays to prove their manufacturability. The obtained OLED displays exhibited a white color EL efficiency that was 27% higher than that of conventional OLED displays.

Acknowledgments

One of authors, Sang-Hwan Cho, would like to thank Min-Kyo Seo at Korea Advanced Institute of Science and Technology (KAIST) for helpful discussion. This work was supported by the Korea Science and Engineering Foundation (KOSEF) (Grant No.ROA-2006-000-10236-0), the Star-Faculty Project (Grant No. KRF-2007-C00018), and the Material Laboratory of Samsung SDI Co., Ltd.

#96549 - $15.00 USD Received 23 May 2008; revised 17 Jul 2008; accepted 31 Jul 2008; published 6 Aug 2008